

dence interval indicates that our present data are not precise enough to pinpoint the mean. As additional data are collected, estimates of the characteristics of the incubation period for AIDS can be improved.

REFERENCES AND NOTES

- J. W. Curran *et al.*, *N. Engl. J. Med.* **310**, 69 (1984).
- C. F. Medley, R. M. Anderson, D. R. Cox, L. Billard, *Nature* **328**, 719 (1987).
- K.-J. Lui *et al.*, *Proc. Natl. Acad. Sci. U.S.A.* **83**, 3051 (1986).
- K.-J. Lui, T. A. Peterman, D. N. Lawrence, J. R. Allen, *Stat. Med.* **7**, 395 (1988).
- K.-J. Lui, T. A. Peterman, D. N. Lawrence, *Nature* **329**, 207 (1987).
- T. A. Peterman, K.-J. Lui, D. N. Lawrence, J. R. Allen, *Transfusion* **27**, 371 (1987).
- M. Rees, *Nature* **326**, 343 (1987).
- D. E. Barton, *ibid.*, p. 734.
- H. J. Alter *et al.*, *Science* **226**, 549 (1984).
- D. P. Francis, *et al.*, *Lancet* **ii**, 1276 (1984).
- M. T. Schreeder *et al.*, *J. Infect. Dis.* **146**, 7 (1982).
- D. P. Francis *et al.*, *Ann. Intern. Med.* **97**, 362 (1982).
- H. W. Jaffe *et al.*, *ibid.* **103**, 210 (1985).
- Centers for Disease Control, *Morbidity and Mortality Weekly Rep.* **36** (no. 2S), 13 (1987).
- D. R. Cox and D. Oakes, *Analysis of Survival Data* (Chapman & Hall, London, 1984).
- A. J. Gross, and V. A. Clark, *Survival Distribution: Reliability Applications in the Biomedical Science* (Wiley, New York, 1975).
- M. Ralston, in *BMDP Statistical Software*, W. J. Dixon, Ed. (Univ. of California Press, Berkeley, 1981), pp. 305–329.
- W. O. Meeker, *Technometrics* **29**, 51 (1987).
- H. Chernoff, *Ann. Math. Stat.* **25**, 573 (1954).
- P. I. Feder, *ibid.* **39**, 2044 (1968).
- If the incubation period of AIDS in homosexual men follows a log-logistic density: $f(t, \theta) = (\lambda\gamma)(\lambda t)^{\gamma-1}/(1 + (\lambda t)^\gamma)^2$, then the estimate \hat{p} of the proportion of infected men who will eventually develop AIDS and the estimate of the median incubation period are 1.00 and 7.9 years, respectively. By the delta method, the mean can also be approximated by 7.9 years. The log-likelihood of this distribution is smaller than that for the Weibull distribution.
- M. G. Koch, *AIDS—from Molecule to Pandemic* (Freeman, New York, 1987).
- J. Seale, *J. R. Soc. Med.* **78**, 613 (1985).
- M. G. Koch, *AIDS-Vår Framtid* (Svenska Carnegie Institutet, Stockholm, 1985).
- P. A. Pålsson, in *Slow Virus Diseases in Animals and Man*, R. H. Kimberlin, Ed. (North-Holland, Amsterdam, 1976), pp. 17–43.
- H. R. Brodt *et al.*, *Dtsch. Med. Wochenschr.* **111**, 1175 (1986).
- J. J. González and M. G. Koch, *Am. J. Epidemiol.* **126**, 985 (1987).
- AIDS Weekly Surveillance Report—United States* (Centers for Disease Control, Atlanta, 1 September 1987).
- We thank W. M. Morgan, H. Jaffe, R. Byers, J. Jason, D. McGee, E. Davis, and M. Kirk for their valuable comments, administrative support, and graphic assistance.

12 November 1988; accepted 5 April 1988

Location and Chemical Synthesis of a Binding Site for HIV-1 on the CD4 Protein

BRADFORD A. JAMESON, PATRICIA E. RAO, LILLY I. KONG, BEATRICE H. HAHN, GEORGE M. SHAW, LEROY E. HOOD, STEPHEN B. H. KENT

The human immunodeficiency virus type 1 (HIV-1) uses the CD4 protein as a receptor for infection of susceptible cells. A candidate structure for the HIV-1 binding site on the CD4 protein was identified by epitope mapping with a family of eight functionally distinct CD4-specific monoclonal antibodies in conjunction with a panel of large CD4-derived synthetic peptides. All of the seven epitopes that were located reside within two immunoglobulin-like disulfide loops situated between residues 1 and 168 of the CD4 protein. The CD4-specific monoclonal antibody OKT4A, a potent inhibitor of HIV-1 binding, recognized a site between residues 32 and 47 on the CD4 protein. By analogy to other members of the immunoglobulin superfamily of proteins, this particular region has been predicted to exist as a protruding loop. A synthetic analog of this loop (residues 25 to 58) showed a concentration-dependent inhibition of HIV-1-induced cell fusion. It is proposed that a loop extending from residues 37 to 53 of the CD4 protein is a binding site for the AIDS virus.

THE AIDS VIRUS, HIV-1, SHOWS A preferential tropism toward helper T cells. The gp120 envelope protein of HIV-1 directly interacts with the CD4 protein of helper T cells (1, 2). Cell surface expression of the CD4 protein on a nonpermissive cell line (HeLa cells) can enable the virus to bind and infect this cell type (3). Monoclonal antibodies to the CD4 protein can prevent HIV-1 from infecting permissive cells (1, 2, 4, 5), and soluble constructs of the CD4 protein are able to inhibit HIV-

1-induced cell fusion (6–10).

The CD4 protein serves as a phenotypic marker for the separation of helper T cells from lymphocyte populations and plays an essential role in the recognition by helper T cells of foreign antigen in the context of the polymorphic class II major histocompatibility complex (MHC) (11). The CD4 protein is encoded by a single gene and is of invariant sequence, in contrast to the class II MHC molecules or the T cell antigen receptor. It is therefore thought that the structure

or structures recognized by the CD4 protein on the MHC is conserved in spite of the polymorphic nature of the MHC. This argument appears to apply to the HIV-1 gp120 as well. The region (or regions) on the gp120 that have been implicated in binding to CD4 reside within highly variable portions of the gp120 (12, 13), yet all known isolates of HIV-1, as well as HIV-2, appear to use the CD4 protein as a receptor and show the same inhibition profiles in response to CD4-specific monoclonal antibodies (14, 15). Furthermore, CD4-specific monoclonal antibodies (mAbs) that block the binding of HIV-1 also inhibit the presentation of foreign antigen and the subsequent stimulation of helper T cells (16–23). This suggests that the same site on CD4 is used both for binding to the class II MHC and to the gp120 of HIV. Thus, identification and characterization of this binding domain on the CD4 is not only important for understanding the virus/receptor interaction, but will aid in the basic understanding of interactions of antigen-presenting cells with helper T cells.

In these studies we used a panel of eight CD4-specific mAbs (Table 1). Antibodies MT-151, OKT4F, and OKT4A are the most potent inhibitors of HIV-1 binding to the CD4 protein, while OKT4D and OKT4E show intermediate inhibitory effects, OKT4B shows only a weak effect, and OKT4 and OKT4C show no effect on virus binding (4, 5, 24). Sattentau *et al.* (5) suggested that two independent binding domains can be discerned by this panel of CD4-specific mAbs, one defined by OKT4A and the other by MT151.

To map the epitopes of the CD4-specific mAbs, we synthesized a panel of CD4-derived peptides (see Fig. 1). We have found that longer peptides (approximately 30 amino acids in length) give more consistent results in direct binding assays than do shorter peptides (6 to 12 amino acids in length) and that antibodies to the longer peptides cross-react better with the native target protein. We therefore used peptides of about 30 amino acids in length. The CD4-specific mAbs were directly assayed for their ability to bind to each synthetic peptide (Fig. 2). Only three of the mAbs consistently recognized any of the CD4-derived peptides in the solid-phase radioimmunoassay (RIA). OKT4C and OKT4F both

B. A. Jameson, L. E. Hood, S. B. H. Kent, Division of Biology, California Institute of Technology, Pasadena, CA 91125.

P. E. Rao, Biotech Division, ORTHO Pharmaceuticals, Raritan, NJ 08869.

L. I. Kong, B. H. Hahn, G. M. Shaw, Division of Hematology/Oncology and Departments of Biochemistry and Microbiology, University of Alabama at Birmingham, Birmingham, AL 35294.

*To whom correspondence should be addressed.

gave reproducible strong signals in the assay, whereas OKT4A, although consistently positive, gave a much weaker signal. OKT4C reacted positively with peptides 18–47 and 25–58. The reaction with peptide 18–47 was consistently the stronger of the two. OKT4A reacted equally well with peptides 18–47 and 25–58. This can be consistently interpreted as follows. Both OKT4C and OKT4A map to the amino-terminal portion of the first disulfide loop of the CD4 protein (see Fig. 1), with OKT4C binding near the amino terminus of 25–58 and to the middle of 18–47, while OKT4A binds toward the middle of both peptides. This implies that OKT4C binds to a region

slightly amino terminal to the OKT4A epitope. OKT4F, which inhibits HIV-1 from binding to the CD4, bound only to peptide 139–168. Thus, this antibody interacts with residues within the second disulfide loop of the CD4 protein (see Fig. 1).

Although neither MT151 nor OKT4B recognized any of the CD4-derived synthetic peptides in the solid-phase RIA, they specifically recognized one peptide in a solution competition binding assay. Each mAb was titrated against a constant number of CD4⁺ CEM cells (8×10^5 cells per well). An antibody concentration ($8 \mu\text{g/ml}$) was selected that was in the presaturation portion of the binding curve and peptide 139–

168 was used to compete (in a concentration-dependent manner) for the binding of the mAb to native CD4 presented on the T-helper lymphocytes (CEM cells). With this assay we were able to map the binding sites of MT151 and OKT4B, and confirm that of OKT4F (Fig. 3). From the data we conclude that OKT4B, OKT4F, and MT151 all bind to the second disulfide loop (139–168).

We then inoculated CD4-derived peptides (25–58, 40–72, 58–93, 111–139, 139–168, and 187–218) into female New Zealand White rabbits. All of the peptides elicited high titers of antibody and, except for the antiserum to peptide 111–139, the antibodies bound specifically to CD4⁺ CEM cells. (The binding of the rabbit anti-

Fig. 1. The panel of CD4-derived synthetic peptides. The heavy line in the center represents the first 218 amino acids of the extracellular domain of the CD4 protein, showing the positions of the first two disulfide loops of the protein as determined by Classon *et al.* (30). The short lines at the top of this figure depict the family of CD4-derived peptides that were synthesized for this study. All of the peptides were synthesized on an Applied Biosystems 430A automated peptide synthesizer according to the procedures of Kent and Clark-Lewis (31) using a paramethylbenzhydrylamine resin (U.S. Biochemicals). Letters at the bottom indicate the relative linear order of the epitopes of the CD4-specific mAbs: OKT4C (C), OKT4A (A), OKT4D (D), OKT4E (E), OKT4 (B), and MT151 and OKT4F (F). The solid lines connecting the various monoclonal antibodies indicate antibodies which displayed reciprocal binding interference patterns in the cross-competition assays.

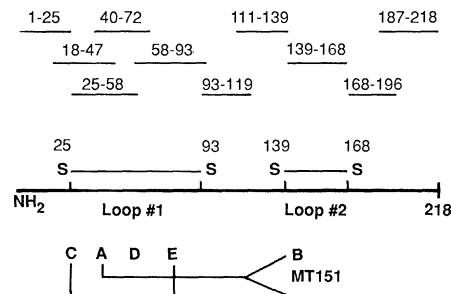


Table 1. The antisera were prepared with an initial intradermal inoculation of keyhole limpet hemocyanin (KLH)-linked peptide (1 mg) mixed 1:1 with Freund's complete adjuvant. Three weeks later, the animals received an intramuscular inoculation of 1 mg of free peptide mixed 1:1 with Freund's incomplete adjuvant. After this, the animals were inoculated in the same manner at 2-week intervals. The antibody titers were measured at 10 weeks after inoculation as described by Emini *et al.* (32). The ability of antisera to bind to native CD4 protein was assayed as described in Fig. 3, except that an ¹²⁵I-labeled goat antibody to rabbit IgG second antibody (ICN Biochemicals) or an FITC-labeled donkey antibody to rabbit IgG second antibody (Jackson Immunologicals) was used. Competition between CD4-specific mAbs and a 1:100 dilution of the rabbit antisera was performed as described in the text. The letters shown in either the RIA or FITC columns refer to the last letter of the mAb for which strong competition (>80% reduction of antibody-CD4 binding) was observed, for example, OKT4A = A. The mAbs that are preceded by three dots were observed to significantly compete with the anti-peptide sera (>40% binding reduction), but to a lesser extent than those antibodies that appear before the three dots. The results shown for syncytia inhibition with respect to the CD4-specific mAbs were taken from McDougal *et al.* (4) and Sattentau *et al.* (5). The antisera were not assayed for cross-reactivity, for example, whether or not anti(25–58) cross-reacts with the peptide 40–72.

Antibody	Anti-CD4 reactivity	Competing monoclonal antibodies		Syncytia inhibition	Solid-phase peptide reactivity	Peptides competing for CD4 binding
		RIA	FITC			
Anti(25–58)	+	A	ND		25–58	
Anti(40–72)	+	ND	D...A, E		40–72	
Anti(58–93)	+	E...D	E		58–93	
Anti(111–139)	–	ND	ND		111–139	
Anti(139–168)	+	B, MT151...F	B		139–168	
Anti(187–218)	+	None	None		187–218	
OKT4	+	ND	None	Negative	None	Negative
OKT4A	+	ND	F, B	Strong	25–58, 18–47	ND
OKT4B	+	ND	A, F	Weak	None	139–168
OKT4C	+	ND	E	Negative	18–47, (25–58)	ND
OKT4D	+	ND	None	Intermediate	None	Negative
OKT4E	+	ND	C	Intermediate	None	Negative
OKT4F	+	ND	A, B	Strong	139–168	139–168
MT151	+	ND	ND	Strong	None	139–168

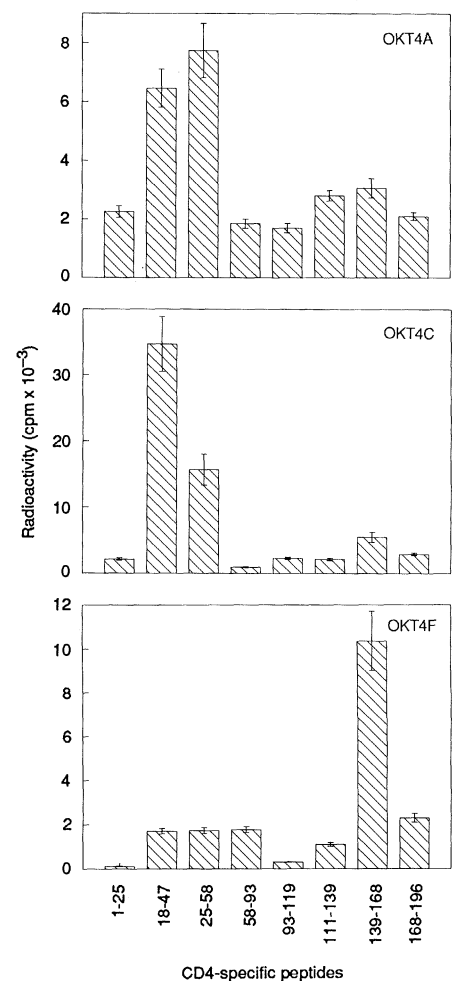


Fig. 2. Solid-phase RIAs of the synthetic peptides with the CD4-specific mAbs OKT4A, OKT4C, and OKT4F. The data show averages of triplicate assays (mean deviation shown by bars; background cpm subtracted). Twenty micrograms of peptide was adsorbed to the bottom of microtiter plates. After washing (tris-buffered saline with 0.1% calf serum), the plates were blocked with 0.1% swine skin gelatin (Sigma) before the addition of the mAb ($20 \mu\text{g/ml}$), according to the procedure of Emini *et al.* (32), except that the binding of the mAbs was monitored with an ¹²⁵I-labeled goat antibody to mouse IgG (ICN Biochemicals).

bodies was monitored either with an ^{125}I - or FITC-labeled second antibody.) Saturating amounts (20 $\mu\text{g}/\text{ml}$) of the CD4-specific mAbs were used to competitively inhibit the binding of each of the rabbit antibodies to the CD4⁺ cells. As shown in Table 1, antibody to peptide 187–218 bound to the native CD4 protein, but was not inhibited by any of the CD4-specific mAbs. Binding of OKT4A to the CD4 protein abolished the binding of anti(25–58), consistent with the data from the solid-phase RIA direct binding assay. OKT4D strongly inhibited the binding of anti(40–72) to CD4 in the fluorescence (FITC) assay. However, the antibodies to 40–72 did not show reproducible binding to the CD4 protein in the RIAs. Incubation of the CD4⁺ cells with OKT4E inhibited the binding of anti(58–93). In the RIAs, OKT4D also inhibited the binding of anti(58–93) but to a lesser extent. These data suggest that OKT4E must bind to the CD4 protein at or very near to the region bound by the antibodies to 58–93, and that OKT4D binds in a region defined by residues 40–72. These data and the direct epitope location data above indicate that the linear order of the epitopes to which the CD4-specific monoclonals bind on the first disulfide loop (see Fig. 1) must be OKT4C, OKT4A, OKT4D, and OKT4E.

The rabbit antibodies to 139–168 were used to confirm the epitope location of OKT4B and MT151. Prior binding of either OKT4B or MT151 inhibited the binding of the anti(139–168) antibodies. Although OKT4F maps to the region 139–168, preincubation of this monoclonal antibody with CD4⁺ cells had only a slight effect on the binding of the anti(139–168) antibodies.

Except for OKT4, which has no effect on HIV-1 binding to T cells, all of the mAbs we tested bind to either the first or second of the amino-terminal disulfide loops (see Fig. 1). This result is consistent with the observations of Traunacker *et al.* (7) that indicate that a truncated soluble CD4 protein consisting only of these two domains is sufficient to competitively inhibit HIV-1 from binding to the CD4 protein.

To obtain information about the steric interactions of the mAbs when bound to the CD4 molecule, each mAb in our panel was FITC-labeled and tested with all members of the panel to probe for binding competitions. The results of these assays are shown in Fig. 4. FITC-OKT4B showed a wide array of competitive binding effects (data not shown). This may be explained by the fact that this protein is a (pentameric) IgM class antibody and is a very large protein complex. All the other members of the panel are

monomeric IgG-type antibodies (24). Of the antibodies tested, only FITC-OKT4 and FITC-OKT4D were unaffected by the binding of the other mAbs. In the other cross-competition studies, only two patterns of reciprocal binding interference were observed. OKT4C and OKT4E exhibited mutually competitive binding while OKT4A, which binds near the amino terminal portion of the first disulfide loop, showed reciprocal competitive binding with the CD4-specific mAbs that we have mapped to the small disulfide loop, 139–168, that is, OKT4F and OKT4B.

Results of the cross-competitions between the various mAbs (Fig. 4) were consistent with the idea that the folded structure of the CD4 protein is such that the two disulfide loops must be close to one another.

Furthermore, the antibodies that exhibit the strongest effects on the ability of HIV-1 to bind to the CD4 protein, that is, OKT4A and OKT4F, must have epitopes that are close to one another and lie in a similar plane so that the bound antibodies interfere with one another. It is significant that data from our solid-phase RIAs show that OKT4A and OKT4C have adjacent epitopes on a linear map (Fig. 1) yet display radically different properties (see Table 1) and do not compete with one another in cross-competition assays, despite the fact that the relative size of each mAb is very large compared to the disulfide loops of the CD4 protein. These geometric implications of the epitope location and competitive binding data can be explained by examining the known three-dimensional structures of proteins related to

Fig. 3. CD4-specific mAb competitions with peptide 139–168. For this assay, the mAbs used were: OKT4A (Δ), OKT4 (\diamond), OKT4F (\blacksquare), OKT4B (\circ) and MT151 (\square). The y-axis shows percentage of mAb bound at various concentrations of the 139–168 peptide. We used 8×10^5 cells per well in a round bottom microtiter plate, and various concentrations of peptide were incubated with 8 $\mu\text{g}/\text{ml}$ of the mAb for 30 min at room temperature before they were added to the CEM cells. The mAb-peptide mixture was allowed to bind for 5 min at room temperature before centrifugation at 1000g for 3 min. The cells were then washed three times for 3 min in a tris-buffered saline solution containing 0.1% calf serum. After washing, the cells were incubated with 10^5 cpm of an ^{125}I -labeled goat antibody to mouse IgG second antibody or, in the case of OKT4B, an ^{125}I -labeled goat antibody to mouse IgM for 15 min at room temperature before washing as described above. At the end of the experiment, the cells were removed from the microtiter plates and radioactivity was monitored in a gamma counter. The data shown here are the averaged results from triplicate assays.

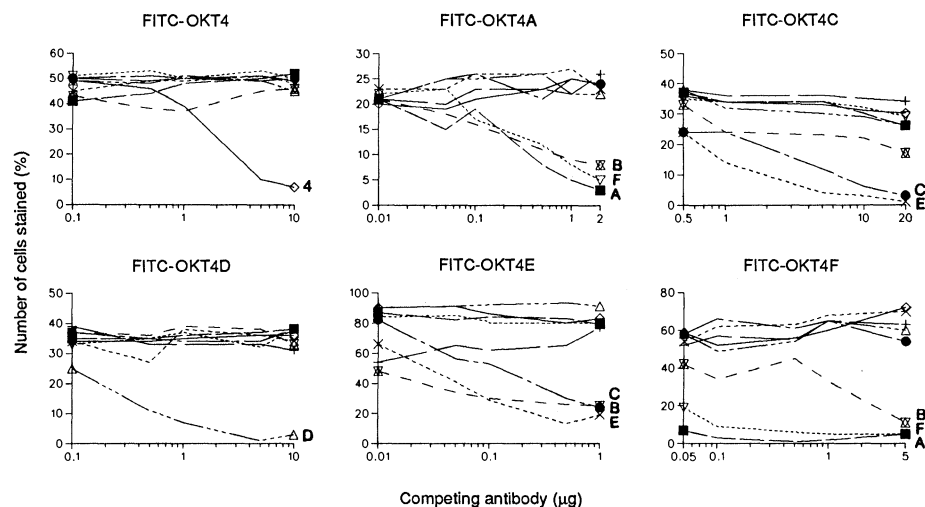
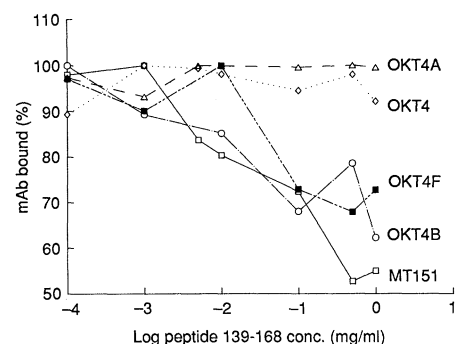


Fig. 4. Cross-competitions within the CD4-specific mAbs. The mAbs OKT4, OKT4A, C, D, E, and F were coupled to FITC and diluted in RPMI with 5% calf serum to concentrations that resulted in slightly subsaturating staining of 5×10^5 PBL or CEM cells. This amount of labeled antibody was then added to 5×10^5 cells in the presence of increasing concentrations of unlabeled mAbs. After 30 min at 4°C, cells were washed free of unbound antibodies in two washes of diluent. Cells were then resuspended in 1 ml of medium and analyzed for fluorescently stained cells on the cytofluorograph. The percent of cells stained by each FITC-coupled antibody is shown in the presence of increasing concentrations of OKT4 (\diamond), OKT4A (\blacksquare), OKT4B (\otimes), OKT4C (\bullet), OKT4D (Δ), OKT4E (\times), or OKT4F (∇).

the CD4 molecule.

The CD4 protein has been classified as a member of the immunoglobulin superfamily of proteins on the basis of sequence similarities, both on the nucleic acid and the amino acid levels (11). It has been suggested that the amino acid sequence alignments and secondary structure predictions indicate that the folding architecture of the family of immunoglobulin-like proteins is highly conserved (25, 26). For this reason, we examined the three-dimensional structures of a series of immunoglobulin regions analogous to residues 1–93 of the CD4 molecule. (The sequence alignments used here in comparing the CD4 protein with the immunoglobulin proteins were derived from published consensus alignments (11, 25, 26).) Figure 5 shows the main chain alpha-carbon backbone of one of those structures, an immunoglobulin light chain variable loop, based on the high resolution x-ray diffraction data of Epp *et al.* (27). We have examined all of the three-dimensional immunoglobulin structures deposited in the Brookhaven Database and, although the exact shape and composition of various loops may differ slightly from one protein to the next, the overall folding architecture is conserved and is exemplified by the human IgG structure shown in Fig. 5.

Immunogenic structures are often found to be loops protruding from the surface of a protein domain. Four protruding loops can be identified in all the CD4-like immunoglobulin structures examined (see Fig. 5). The assignment of these four loops to the epitopes for OKT4C, OKT4A, OKT4D, and OKT4E, respectively, is consistent with our epitope location data. Furthermore, cross-competition studies with OKT4C and OKT4E indicated that their respective epitopes must be spatially close and oriented such that bound mAbs interfere with one another. In Fig. 5, the blue (OKT4C) and orange (OKT4E) loops fulfill these criteria. The red loop (Fig. 5) assigned to OKT4A, neighbors the blue loop assigned to OKT4C, yet the two loops are oriented in opposite directions, consistent with our observation that OKT4A and OKT4C do not cross-compete. Finally, the green loop (OKT4D) protrudes in such a way that an antibody binding to this loop would not be expected to interfere with the binding of any of the other antibodies. These data strengthen the notion that the three-dimensional structure of the first 93 amino acids of the CD4 protein is analogous to the corresponding region of the immunoglobulin structure.

We may now reach certain conclusions concerning the CD4 interactions with HIV-1. The red loop (Fig. 5) protrudes well away

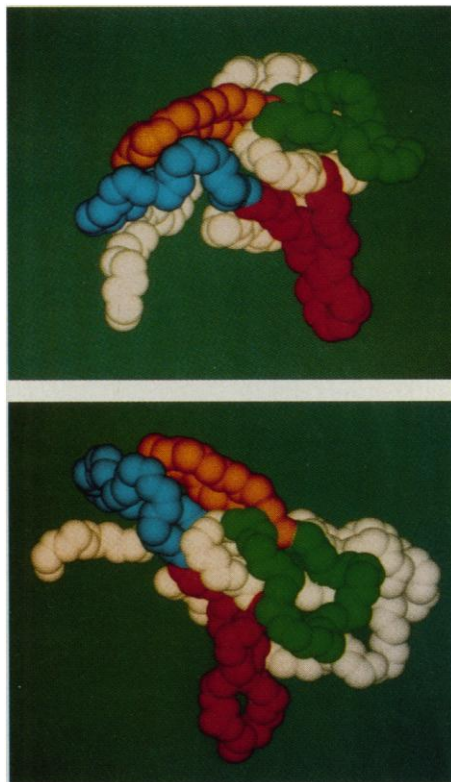


Fig. 5. Two views of the structure of an immunoglobulin variable loop domain. The structure shown here is that of the α -carbon backbone of Fab fragment light chain, residues 1–88 (27). The crystal coordinates were obtained from the Brookhaven Database (database code: IREI). The image was constructed by use of the Biograf program, version 1.4 (BioDesign). The blue loop, light chain residues 23–33, is analogous to CD4 residues 25–35; the red loop, light chain residues 35–47, is analogous to CD4 residues 37–53; the green loop, light chain residues 52–63, is analogous to CD4 residues 58–68; the orange loop, light chain residues 64–73, is analogous to CD4 residues 70–79. The blue and orange loops shown here represent the antigen-combining loops of this light chain structure.

from its surrounding chains such that it looks like an extended finger. An antibody to this “finger” (OKT4A) would prevent HIV-1 from binding to the CD4 protein, whereas an antibody binding to the blue loop, which is adjacent but points in the opposite direction, would have no effect on the binding of HIV-1. The observation that anti-idiotypes of OKT4A bind to the outer envelope of HIV-1 (28) suggests that the binding inhibition observed with OKT4A is not due simply to neighboring steric effects, but rather that at least portions of the OKT4A epitope are directly involved in the attachment of HIV-1 to the CD4 protein. By analogy with the picornaviruses (29), and according to the suggestion of Lasky *et al.* (13), it seems likely that the receptor attachment site on the surface of the HIV-1 occurs as a valley or invagination. Thus, our data suggest that CD4 residues 37–53 (see

the red loop, Fig. 5) form a finger-like projection from the surface of the CD4 protein that serves as a binding site for HIV-1.

We therefore tested the CD4-derived synthetic peptide 25–58 in an HIV-1-induced cell fusion (syncytium formation) assay using HIV-1/WMJ-infected cells mixed (1:5) with uninfected SupT1 cells. This peptide specifically inhibited syncytium formation in a concentration-dependent manner, down to concentrations of 200 μ g/ml. Peptides 1–25 and 40–72 were used as controls, but neither inhibited the virus-induced cell fusion at equivalent concentrations. When peptide 25–58 was washed from the assay after 2 hours, syncytium formation proceeded normally, indicating that the peptide was not exerting a toxic effect on the cells and that the observed inhibition was due solely to the presence of the 25–58 peptide.

Peptide analogs of the CD4 region 37–53 may be useful to more precisely determine the fine structure of the HIV-binding site, and may ultimately lead to the design of small molecule inhibitors of the AIDS virus-receptor interaction.

REFERENCES AND NOTES

1. A. G. Dalgleish *et al.*, *Nature* **312**, 763 (1984).
2. D. Klatzmann *et al.*, *ibid.*, 767.
3. P. J. Maddon *et al.*, *Cell* **47**, 333 (1986).
4. J. S. McDougal *et al.*, *J. Immunol.* **137**, 2937 (1986).
5. Q. J. Sattentau, A. G. Dalgleish, R. A. Weiss, P. C. L. Beverley, *Science* **234**, 1120 (1986).
6. D. H. Smith *et al.*, *ibid.* **238**, 1704 (1987).
7. A. Trauncker, W. Luke, K. Karjalainen, *Nature* **331**, 84 (1988).
8. R. E. Hussey *et al.*, *ibid.*, p. 78.
9. K. C. Deen *et al.*, *ibid.*, p. 82.
10. R. A. Fisher *et al.*, *ibid.*, p. 76.
11. D. R. Littman, *Annu. Rev. Immunol.* **5**, 566 (1987).
12. M. Kowalski *et al.*, *Science* **237**, 1351 (1987).
13. L. A. Lasky *et al.*, *Cell* **50**, 975 (1987).
14. A. G. Dalgleish, B. J. Thomson, T. C. Chan, M. Malkovsky, R. C. Kennedy, *Lancet* **ii**, 1047 (1987).
15. H. Kornfield, N. Riedel, G. A. Viglianti, V. Hirsch, J. I. Mullins, *Nature* **326**, 610 (1987).
16. W. E. Biddison, P. E. Rao, M. A. Talle, G. Goldstein, S. Shaw, *J. Exp. Med.* **156**, 1065 (1982).
17. ———, *J. Immunol.* **131**, 152 (1983).
18. ———, *J. Exp. Med.* **159**, 783 (1984).
19. L. Rogozinski *et al.*, *J. Immunol.* **132**, 735 (1984).
20. P. G. Coulter, J. P. Coutelier, C. Uytendhove, P. Lambotte, J. Van Snick, *Eur. J. Immunol.* **15**, 638 (1985).
21. B. P. Sleckman *et al.*, *Nature* **328**, 351 (1987).
22. K. Krohn, W. G. Robey, S. Putney, M. A. Talle, A. Ranki, in *Vaccines 87*, R. M. Chanock, R. A. Lerner, F. Brown, H. Ginsberg, Eds. (Cold Spring Harbor Laboratory, Cold Spring Harbor, NY, 1987), pp. 225–230.
23. D. Wernicke-Jameson, P. Rao, B. A. Jameson, S. B. H. Kent, unpublished observations.
24. The isotypes of the monoclonal antibodies are as follows: OKT4 = γ 2b; OKT4A = γ 2a; OKT4B = μ ; OKT4C = γ 2a; OKT4D = γ 1; OKT4E = γ 1; OKT4F = γ 1; and MT151 = γ 1.
25. S. J. Clark *et al.*, *Proc. Natl. Acad. Sci. U.S.A.* **84**, 1149 (1987).
26. A. F. Williams, *Immunol. Today* **8**, 298 (1987).
27. O. Epp *et al.*, *Biochemistry* **14**, 4943 (1975).
28. R. C. Kennedy *et al.*, *Third International Conference on AIDS*, Washington, DC (1987), p. 160.
29. J. M. Hogle, M. Chow, D. J. Filman, *Science* **229**, 1358 (1985).
30. B. J. Classon, J. Tsagaratos, I. F. C. McKenzie, I. D.

Walker, *Proc. Natl. Acad. Sci. U.S.A.* **83**, 4499 (1986).

31. S. Kent and I. Clark-Lewis, *Synthetic Peptides in Biology and Medicine*, K. Alitalo, P. Partanen, A. Vaheri, Eds. (Elsevier, New York, 1985), pp. 29–58.
32. E. A. Emini, B. A. Jameson, E. Wimmer, *Nature* **304**, 699 (1983).
33. Principal support for this work was provided by a Marshall Field's Award from the American Founda-

tion for AIDS Research, grant No. 00465R (S.B.H.K.). The cell fusion assays were supported by AI25784 (G.S. and B.H.). We thank P. Rieber for MT151, D. Wernicke-Jameson for discussions, P. Dervan for the use of computer facilities, S. Perry, E. McAnaney, and L. Martin Selk for technical assistance, C. Elkins for manuscript typing, and D. Noskowitz for figure preparation.

18 February 1988; accepted 18 April 1988

Expression of the β -Nerve Growth Factor Gene in Hippocampal Neurons

CHRISTIANE AYER-LELIEVRE,* LARS OLSON, TED EBENDAL, ÅKE SEIGER, HÅKAN PERSSON

In situ hybridization with complementary DNA probes for nerve growth factor (NGF) was used to identify cells containing NGF messenger RNA in rat and mouse brain. The most intense labeling occurred in hippocampus, where hybridizing neurons were found in the dentate gyrus and the pyramidal cell layer. The neuronal identity of NGF mRNA-containing cells was further assessed by a loss of NGF-hybridizing mRNA in hippocampal areas where neurons had been destroyed by kainic acid or colchicine. RNA blot analysis also revealed a considerable decrease in the level of NGF mRNA in rat dentate gyrus after a lesion was produced by colchicine. This lesion also caused a decrease in the level of Thy-1 mRNA and an increase in the level of glial fibrillary acidic protein mRNA. Neuronal death was thus associated with the disappearance of NGF mRNA. These results suggest a synthesis of NGF by neurons in the brain and imply that, in hippocampus, NGF influences NGF-sensitive neurons through neuron-to-neuron interactions.

NERVE GROWTH FACTOR (NGF) IS essential in the development and maintenance of sympathetic and sensory peripheral neurons (1). In the central nervous system, cholinergic neurons of the septum-basal forebrain respond to exogenous NGF by increasing the levels of choline acetyltransferase (2), and the target areas of these neurons (hippocampus and cortex) contain the highest levels of NGF mRNA in the brain (3). Septum-basal forebrain neurons also carry NGF receptors (4), can retrogradely transport exogenous NGF injected into the hippocampus (5), and can be prevented from dying after axonal transection by infusion of NGF (6).

The structure of the NGF precursor pro-

tein has been deduced from DNA sequence analysis of cloned NGF genes (7–9). NGF mRNA has been detected in the brain of several species, including rat (3), but the cell types that synthesize NGF in the central nervous system are not known. In the study described here, we used in situ hybridization and RNA blot analysis in normal rats and in rats with experimental lesions to identify NGF mRNA-containing cells in the rodent brain.

In situ hybridization was performed with a ^{32}P -labeled 900-bp Pst I fragment from a mouse NGF cDNA clone. This fragment shows 97% DNA sequence homology between mouse and rat (9) and hybridizes strongly to rat NGF mRNA under stringent conditions (3). Under the conditions we used, a strong labeling occurred over NGF mRNA-containing cells in male mouse submandibular glands (10). In rat and mouse brain, the NGF cDNA probe revealed NGF mRNA in the dentate gyrus and in the hippocampal pyramidal cell layer in areas CA1 to CA4 (Fig. 1A). The same hybridization pattern was also seen when the NGF probe was mixed with an excess of unlabeled pUC9 DNA to eliminate possible nonspecific labeling over the hippocampus. Furthermore, a nonoverlapping NGF cDNA fragment, covering the 3' untranslated re-

gion, showed an identical hybridization pattern, thus providing evidence against a nonspecific cross-hybridization of the probes with mRNA other than NGF mRNA.

Hybridization with a 900-bp Pst I fragment from the chicken NGF gene, corresponding to the 900-bp fragment of mouse cDNA, gave only weak labeling on male mouse submandibular gland (10) and no labeling on sections of rat brain. This result is consistent with previous RNA blot analysis that showed limited cross-hybridization between mouse NGF mRNA and chicken NGF probes under high stringency conditions of hybridization (8). No hybridization was observed when pUC9 DNA was used as a hybridization probe or after treatment of sections with ribonuclease A (RNase A). Furthermore, under the same hybridization conditions, unrelated cDNA probes for genes expressed in rat and mouse brain gave

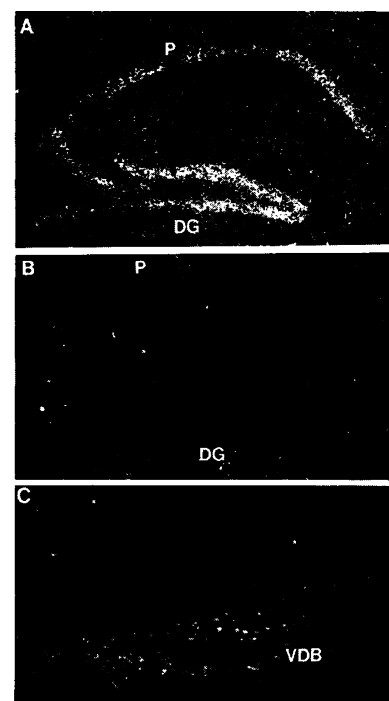


Fig. 1. In situ hybridization to sections of rat hippocampus. The DNA probes were labeled with [α - ^{32}P]deoxycytidine 5'-triphosphate (dCTP) by nick translation to a specific activity of approximately 10^9 cpm/ μg , and 5 to 10 ng of probe were added to each section. The conditions for in situ hybridization were as described (10, 23). The slides were dehydrated and dipped in 50% Ilford K5 nuclear emulsion and exposed for 9 days. The following probes were used: (A) A 900-bp Pst I fragment from a mouse NGF cDNA clone (7) and (B and C) a 400-bp Bst EII fragment derived from a rat NGF receptor cDNA clone (24). (A and B) Sagittal sections of rat brain at hippocampus level. (C) Transverse section through the ventral part of vertical limb of diagonal band of Broca (VDB). The sections are shown in dark-field illumination ($\times 18$). Abbreviations: P, pyramidal cell layer, and DG, granular cell layer of dentate gyrus.

C. Ayer-LeLievre, Department of Medical Chemistry, Laboratory of Molecular Neurobiology, and Department of Histology and Neurobiology, Karolinska Institutet, Box 60400, S-104 01 Stockholm, Sweden.

L. Olson, Department of Histology and Neurobiology, Karolinska Institutet, Box 60400, S-104 01 Stockholm, Sweden.

T. Ebendal, Department of Developmental Biology, Uppsala University, P.O. Box 587, S-751 23 Uppsala, Sweden.

Å. Seiger, Department of Neurological Surgery, University of Miami School of Medicine, Miami, FL 33136.

H. Persson, Department of Medical Chemistry, Laboratory of Molecular Neurobiology, Karolinska Institutet, Box 60400, S-104 01 Stockholm, Sweden.

*To whom correspondence should be addressed at the Department of Histology and Neurobiology, Karolinska Institutet, Box 60400, S-104 01 Stockholm, Sweden.